REPORT DOCUMENTATION PAGE

Form Approved
OMB No. 0704-0188

1. REPORT DATE *(DD-MM-YYYY)*	2. REPORT TYPE	3. DATES COVERED *(From - To)*
31-03-2010	Final Technical	15-01-2007 - 31-12-2009

4. TITLE AND SUBTITLE

(U) DISPERSION, MIXING, AND COMBUSTION IN TURBULENT AND HIGH-SPEED FLOWS, AIR-BREATHING PROPULSION, AND HYPERSONIC FLIGHT

5a. CONTRACT NUMBER

5b. GRANT NUMBER
FA9550-07-1-0091

5c. PROGRAM ELEMENT NUMBER
61102F

6. AUTHOR(S)

Paul E. Dimotakis, Daniel I. Meiron

5d. PROJECT NUMBER
2308

5e. TASK NUMBER
BX

5f. WORK UNIT NUMBER

7. PERFORMING ORGANIZATION NAME(S) AND ADDRESS(ES)

Mail Code 301-46
California Institute of Technology
1200 East California Blvd.
Pasadena CA 91125

8. PERFORMING ORGANIZATION REPORT NUMBER

None

9. SPONSORING / MONITORING AGENCY NAME(S) AND ADDRESS(ES)

Air Force Office of Scientific Research
875 North Randolph Street
Suite 325, Room 3112
Arlington VA 22203-1768

10. SPONSOR/MONITOR'S ACRONYM(S)

11. SPONSOR/MONITOR'S REPORT NUMBER(S)
AFRL-AFOSR-VA-TR-2016-0678

12. DISTRIBUTION / AVAILABILITY STATEMENT

Approved for public release. Distribution is unlimited.

13. SUPPLEMENTARY NOTES

14. ABSTRACT

The research studied the dispersion and mixing in turbulent flows with applications to high-speed, air-breathing propulsion. Experiments investigating molecular mixing in high-speed internal flows demonstrated that fuel injection through a perforated inclined ramp can lead to considerable mixing enhancement compared to free-shear layers, with small attendant total-pressure losses. Numerical large-eddy simulations (LES) with subgrid-scale (SGS) modeling successfully captured the large-scale features of this flow (except for near-wall separation), the observed recirculating flow, chemical product formation under lean- and rich-reactant conditions, and molecular mixing for the first time. A modification will enable investigations of inclined-jet injection, with and without a downstream shear layer. As part of the research on hydrocarbon flames, a new facility was designed and fabricated. Preliminary experiments demonstrated stable flame operation at pressures in excess of 5 atm. Separate investigations of scalar dispersion and mixing in grid turbulence elucidated the importance and role of injection details through their influence on the characteristics of the resulting flow.

15. SUBJECT TERMS
High-speed flow, air-breathing propulsion, dispersion, mixing, turbulence.

16. SECURITY CLASSIFICATION OF:			17. LIMITATION OF ABSTRACT	18. NUMBER OF PAGES	19a. NAME OF RESPONSIBLE PERSON
a. REPORT	b. ABSTRACT	c. THIS PAGE			Dr. Julian Tishkoff
Unclassified	Unclassified	Unclassified	UL	29	19b. TELEPHONE NUMBER *(include area code)* 703-696-8478

GRADUATE AERONAUTICAL LABORATORIES
CALIFORNIA INSTITUTE OF TECHNOLOGY
Pasadena, California 91125

DISPERSION, MIXING, AND COMBUSTION IN TURBULENT AND HIGH-SPEED FLOWS, AIR-BREATHING PROPULSION, AND HYPERSONIC FLIGHT

Paul E. Dimotakis (PI), Caltech
Daniel I. Meiron (Co-PI), Caltech

Air Force Office of Scientific Research
Grant FA9550-07-1-0091

Final Technical Report
15 January 2006 – 31 December 2009

31 March 2010, edited 21 May 2010

Summary/Overview

This is the final report on research combining experiments, numerical simulations, modeling, and instrumentation-development from 15 January 2007 to 31 December 2009. The research studied the dispersion and mixing in turbulent flows with applications to high-speed, air-breathing propulsion. Experiments investigating molecular mixing in high-speed internal flows demonstrated that fuel injection through a perforated inclined ramp can lead to considerable mixing enhancement compared to free-shear layers, with small attendant total-pressure losses. Numerical large-eddy simulations (LES) with subgrid-scale (SGS) modeling successfully captured the large-scale features of this flow (except for near-wall separation), the observed recirculating flow, chemical product formation under lean- and rich-reactant conditions, and molecular mixing for the first time. A modification will enable investigations of inclined-jet injection, with and without a downstream shear layer. As part of the research on hydrocarbon flames, a new facility was designed and fabricated. Preliminary experiments demonstrated stable flame operation at pressures in excess of 5 atm. Separate investigations of scalar dispersion and mixing in grid turbulence elucidated the importance and role of injection details through their influence on the characteristics of the resulting flow.

Much of the research conducted during this period derives from and builds on previous work under AFOSR Grant FA9550-04-1-0020, and benefitted from collaborations with U. Minnesota, CUBRC, and Virginia Tech MURI program partners under AFOSR Grant FA9550-04-1-0389 with which it overlapped in time (1 Jun 2004 – 31 May 2009) and focus in some areas. It also benefitted from progress in computational fluid dynamics realized under the Department of Energy (DOE)-funded Advanced Scientific Computing (ASC) Alliance Center at Caltech (PI: Dan Meiron) under Subcontract No. B341492 of DOE contract W-7405-ENG-48. The research and progress on scalar dispersion would not have been possible without instrumentation and data-acquisition equipment contributions developed under support by the National Science Foundation (NSF) Major Research Instrumentation (MRI) Grant EIA-0079871 (1 Sep 2000 – 31 Aug 2004).

Technical discussion

Research conducted under this grant focused in three interrelated areas: mixing and combustion in high-speed flows, hydrocarbon combustion and flames, and scalar dispersion in a turbulent-flow environment. Results from this work are documented in the discussion below.

Mixing and combustion in high-speed flows

The aim of this part of the research is to probe and understand some of the fundamental issues related to mixing and combustion in high-speed air-breathing propulsion systems. Specifically, the research investigated fuel injection and mixing in complex, accelerating-flow environments, with high density gradients, the effect of finite chemical kinetics over variable pressures, and combustion and heat release. The investigations extend into internal flows ranging from the high-speed subsonic regime to flows at $M_1 = 1.5$ and $M_1 = 2.5$, where M_1 is the upper (high-speed) stream Mach number, with and without inclined-jet injection, both with and without chemical reactions and heat release. The

research entailed a combination of successful experimental investigations, in concert with detailed large-eddy simulations (LES) in concert with subgrid-scale (SGS) modeling.

Experimental work

This part of the research focused on experimental investigations, the development of necessary instrumentation and diagnostic techniques, as well as simulation of the three-dimensional compressible flows that ensue, including those flows related to inclined-jet injection in air-breathing propulsion applications.

Initial experimental work on compressible turbulent mixing under this grant was centered on studying the flow control and mixing achieved in a low total-pressure-loss, expansion ramp geometry (Fig. 1) that was first developed under a previous AFOSR core-program grant (FA9550-04-1-0020) and extended its capabilities with support derived from the AFOSR MURI program (FA9550-04-1-0389) funds, as discussed below.

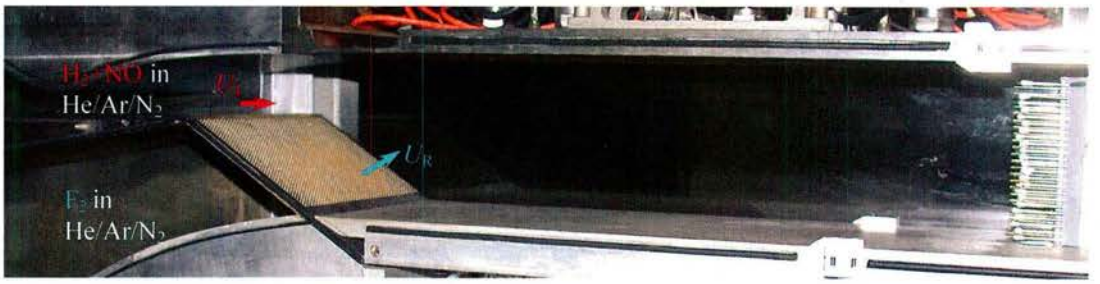

Fig. 1. The previous supersonic shear-layer facility expansion-ramp flow geometry

In the geometry investigated, a high-speed upper (nominally) "air" stream is expanded over a ramp inclined at 30° to the flow. A low-speed "fuel" stream is injected through perforations in the ramp and generates a mixing layer between the two streams. A key feature of this flow is a purposely-designed recirculation zone that transports hot products back toward the fuel injection location and provides a low-strain-rate flameholding region (Johnson 2005, Bergthorson *et al.* 2007).

Figure 2 shows a composite (spliced) schlieren image from a pair of experiments with a $M_1 = 1.5$ upper stream flow and a lower stream injection with a ramp velocity of $U_R = 5$ m/s. The flow expands down the ramp, creating a perturbed (enhanced entrainment) mixing layer that interacts with waves reflected off the upper guidewall. The adverse pressure gradient results in separation of the top-wall boundary layer upstream of the measurement rake. As found for a subsonic top-stream, this flow can be controlled by varying the mass injected through the perforated ramp. Figure 3 is a composite schlieren image for a lower stream injection of $U_R = 45$ m/s and the same top-stream conditions, illustrating the efficacy of the control that can be exercised.

The shear layer can be seen to be almost horizontal, indicating that streamwise pressure gradients are nearly eliminated, the upper-stream wave system remains uniform, and no boundary-layer separation occurs. A measure of the aerodynamic performance of the device is the overall pressure coefficient, $Cp = 2\,(p_e - p_i) / (\rho\, u^2)$, where p_e and p_i are the exit/exhaust and inlet pressures, respectively, and $\rho\, u^2/2$ is the dynamic pressure.

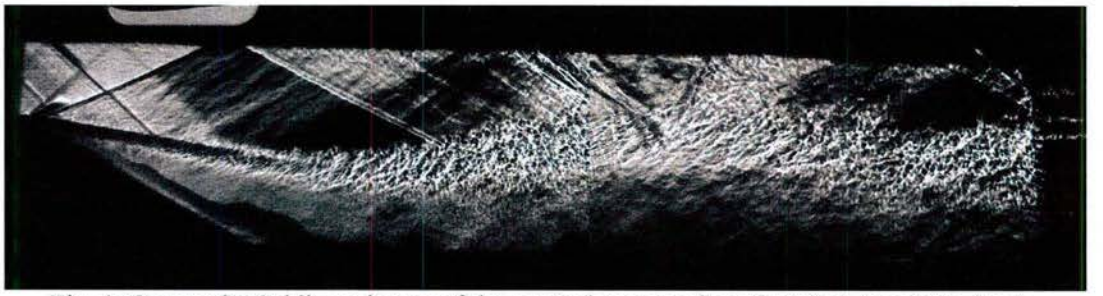

Fig. 2. Composite Schlieren image of the expansion-ramp flow for M_1=1.5 and U_R=5 m/s.

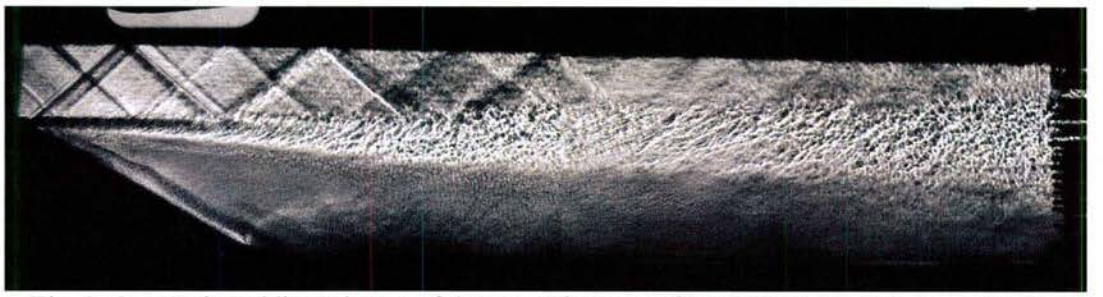

Fig. 3. Composite schlieren image of the expansion-ramp flow for M_1 = 1.5 and U_R = 45 m/s.

Measured pressure coefficients are plotted in Fig. 4 for the M_1 = 1.5 (diamonds) and 2.5 (circles) supersonic-flow experiments conducted with variable injection and heat release. The slope of this profile has the opposite sign as for subsonic flow (Johnson 2005, filled symbols), as would be expected for one-dimensional compressible flow that provides an adequate simplification of the pressure behavior in this respect. Similarly to the subsonic-flow results (Johnson 2005), mass injection exerts significant control authority.

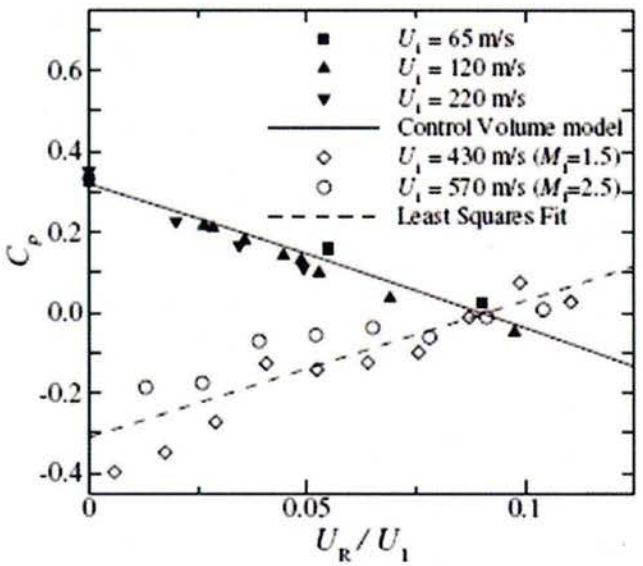

Fig. 4. Measured overall pressure coefficient vs. mass-injection ratio and chemical heat release.

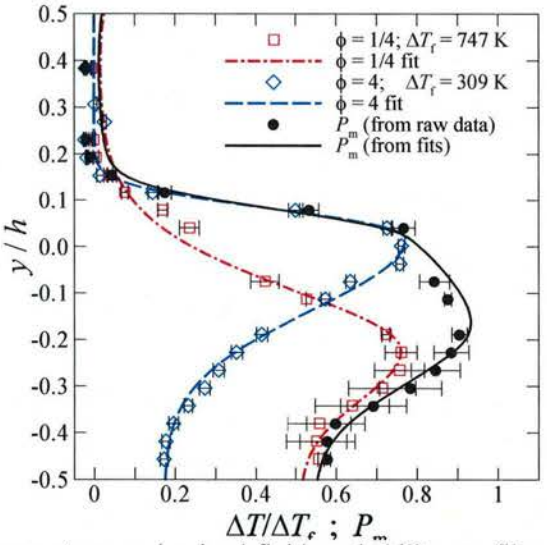

Fig. 5. Normalized temperature and mixed-fluid probability profiles for flip experiments at $M_1 = 2.5$ and $U_R = 60$ m/s.

Heat release allows the same pressure coefficient to be achieved with a mass injection almost a factor of four lower than for non-reacting flow (Bergthorson *et al.* 2007, Bonanos *et al.* 2008). Molecular scale mixing was measured using the "flip" experiment technique (Mungal and Dimotakis 1984, Dimotakis 2005). Mixing measurements in this flow geometry were completed at various speeds, up to a top stream Mach number of $M_1 = 2.5$. For a top-stream Mach number of $M_1 = 1.5$ and a velocity ratio $U_R/U_1 = 0.1$, an estimated 44% of fluid in the duct was mixed at a molecular scale after 4.3 duct heights, and 58% was mixed after 5.4 duct heights. For $M_2 = 2.5$ and $U_R/U_1 = 0.1$, an estimated 47% of fluid was (molecularly) mixed after 5.4 duct heights. Normalized temperature-rise profiles for the two flip experiments and the estimated probability profile for mixed fluid for $M_1 = 2.5$ flow are shown in Fig. 5 (Bonanos *et al.* 2008). The previously observed trends of decreasing levels of molecular mixing with increasing flow speed (upper-stream velocity) persist.

To explore further increases in molecular mixing, the facility was modified to accommodate transverse jets in the upper (high-speed) flow. These jets can excite additional instabilities in the shear layer and enhance mixing. The modified facility can accommodate adjustable ramp heights and variations in ramp-injection mass fluxes.

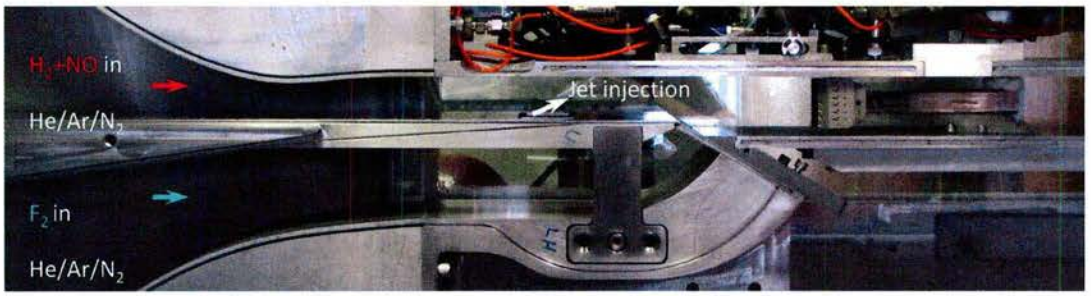

Fig. 6. The new Supersonic Shear Layer (S3L) facility test section incorporates a modular injector block. Mass injection and momentum flux through angled jets can be varied to influence shear-layer entrainment prior to reattachment, providing additional mixing enhancement/control.

The modified test section (Fig. 6) enables the investigation of several injector configurations. In addition, the boundary-layer thickness of the incoming flow, which is an important parameter in a scramjet combustor, can potentially be controlled via injection through a perforated plate. These modifications will enable the exploration of the effects of inclined-jet injection on mixing and combustion, while creating a valuable data set that would be important in support of code development and validation.

The injector fits into the splitter plate of the S3L wind-tunnel shown in Figs. 6 and 7. The diamond injectors have a long dimension of 12.7 mm (0.5 in) and a short dimension of 2.3 mm (0.09 in). The round injectors have a diameter of 3 mm (0.12 in). The injector insert developed under this grant is shown in Fig. 8. The depicted geometry consists of five jets (two diamond and three circular) transversely angled at 30° relative to the downstream direction. This configuration was chosen based on the experience and work by Schetz and coworkers (e.g., Barber *et al.* 1997). The equidistant alternation between diamond and circular injectors has a centered circular injector.

Non-reactive flow experiments were performed at a nominal top-stream Mach number of $M_1 = 1.5$. Freestream conditions were fixed at a total pressure of 300 kPa and total temperature of approximately 295 K. The lower stream was set to a ramp injection velocity of $U_R = 8.5$ m/s. Nitrogen was used as the injectant with a sonic injection Mach number. The jet-to-freestream momentum flux ratio, $\bar{q} \equiv (\rho\, U^2)_j / (\rho\, U^2)_1$, quantifies the control exerted by the injector. The present injector array, at $\bar{q} = 2$, resulted in an injected mass-flow rate through the ramp of $\dot{m}_R = 84$ g/s.

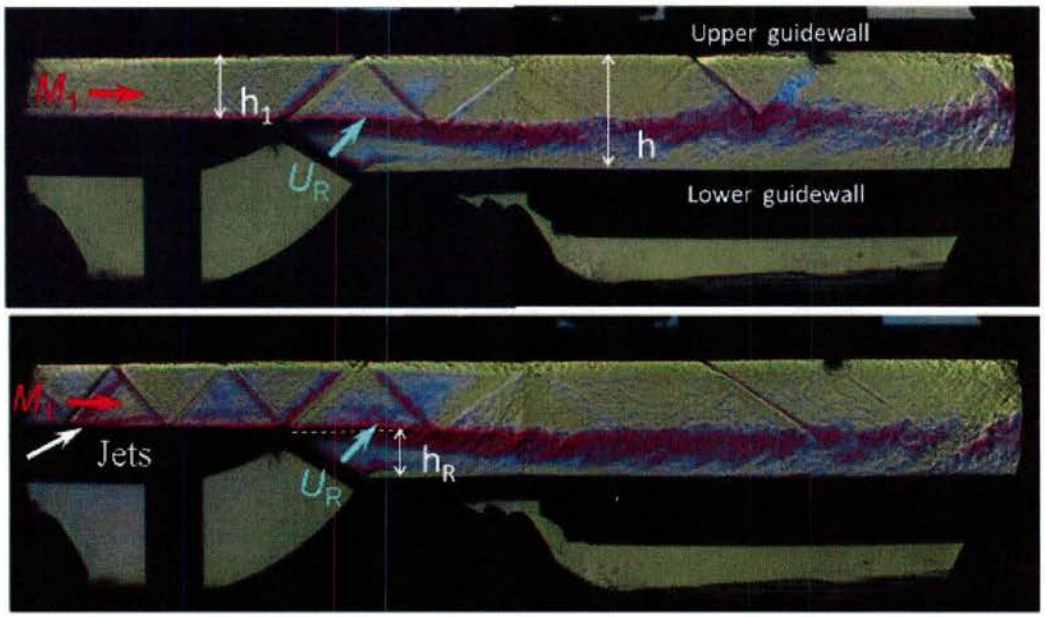

Fig. 7. Typical composite schlieren images obtained in the modified test section and nomenclature. Top: Ramp-injection only (without jet injection). Bottom: Combined ramp and inclined-jet injection. Both upper and lower streams are 100% [N_2].

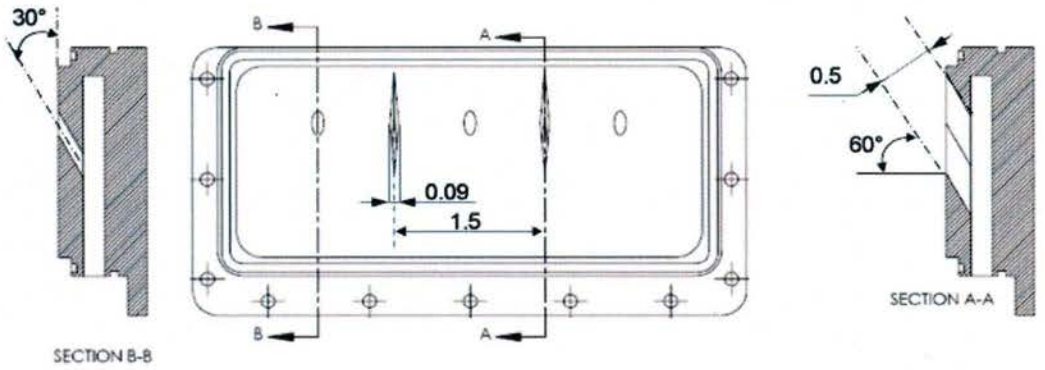

Fig. 8. Jet-injector insert detail. Dimensions given in inches.

Diagnostics included upper- and lower-guidewall pressure transducers that registered pressure at taps installed along the top guidewall, as well as in the upper- and lower-stream plena. During a run, data were recorded at a rate of 1 kHz/channel through a National Instruments LabView hardware/software data-acquisition and control system. The schlieren imaging system employed a nanosecond duration light source (MiniStrobokin power supply with K-L lamp) and a high-speed CMOS camera (Phantom v7.1) operated at framing rates up to 1000 fps. The schlieren system was mounted to rails that allowed translation and imaging of different portions of the test section.

Experiments, conducted at moderate compressibility ($M_1 = 1.5$) in a non-reacting environment, illustrate some of the phenomenology associated with transverse-jet injection and shear layer interaction. Schlieren side-view images of these experiments with $U_1 = 430$ m/s ($\dot{m}_1 = 3$ kg/s) top-stream flow and a ramp-injection velocity of $U_R = 8.5$ m/s ($\dot{m}_2 = 0.15$ kg/s) are shown in Figs. 9a and 9b.

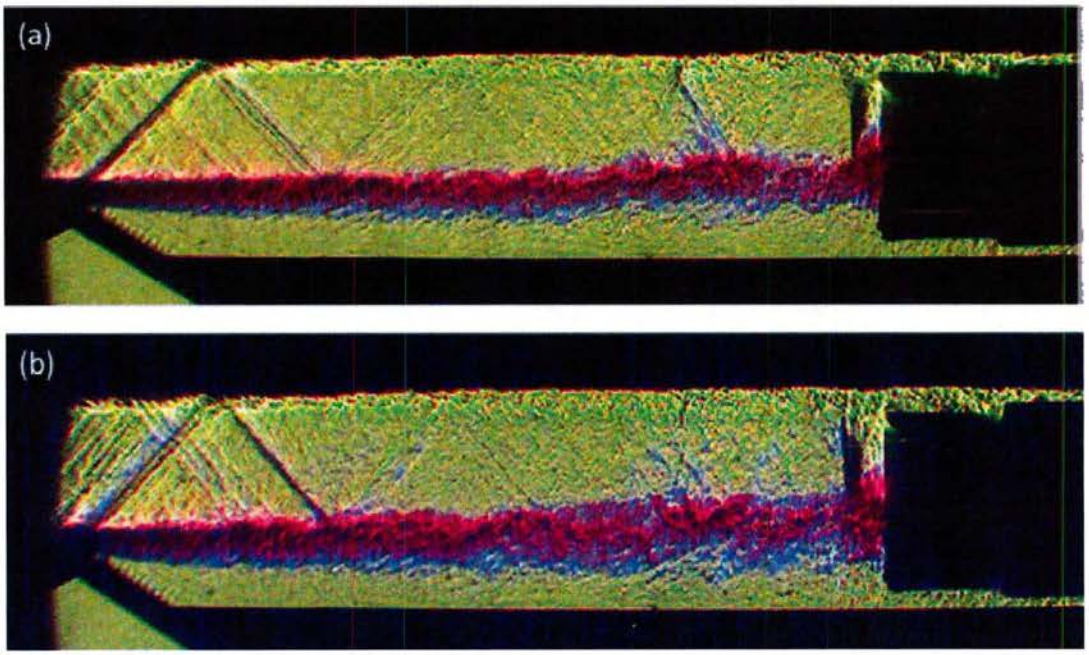

Fig. 9. Color schlieren image data. a) No Jet injection. b) Inclined jet injection at $\overline{q} = 2$.

The flow depicted in the schlieren images in Fig. 9 are with ramp injection and (a) no jets, as well as (b) with inclined-jet injection. Figure 9a depicts spliced instantaneous side-view schlieren images for a flow configuration with ramp injection only (no jet injection). Figure 9b depicts side-view schlieren data with jet injection at a jet-to-freestream momentum flux ratio of $\bar{q} = 2$.

Jet injection (Fig. 9b) is found to be responsible for an increase in the mixing-layer transverse extent (thickness), compared to the no-jet-injection case (Fig. 9a). The initial mixing layer behavior does not change significantly, leading to the inference that the increased thickness is attributable to an enhancement in growth rate (entrainment) with downstream distance. The difference between the two flows is registered in the difference between the stand-off shock in front of the probe array, with the shock closer to the probes with no jet injection, as compared to the flow with jet injection.

Based on results in non-reactive flows, injector geometries will be selected and investigated in reacting flows in the future. We anticipate that the documented increase in shear-layer entrainment and mixing will be augmented by that resulting from the flow from the inclined jets themselves to yield a substantially increased overall amount of molecularly mixed fluid in the combustor duct, with minimal (additional) total-pressure losses. A new instrumentation rake will be used to measure the temperature field. Mach number and total pressure will be measured using the micro-probe technology documented previously (Maddalena *et al.* 2008a).

Following the test section upgrade, a successful supersonic ($M_1 = 1.5$) shear-layer run with reactive jets (Top: 1.95% [H2]; Bottom: 0.1% [NO], 2% [F2]) was performed, with a bottom-to-top stream mass-flow ratio of 0.12.

The injected transverse jets interact with the primary shear layer to produce a three-dimensional flow with moderate swirl. The old rake that was designed to make measurements in configurations that produced two-dimensional flows with little spanwise variation cannot be used to capture the new flow-field features. A new thermocouple rake with 40 channels organized as an 8×5 array was designed. The rake design (Fig. 10) takes the global and local blockage effects in the test-section into account to avoid choking, i.e., driving the flow to locally sonic conditions.

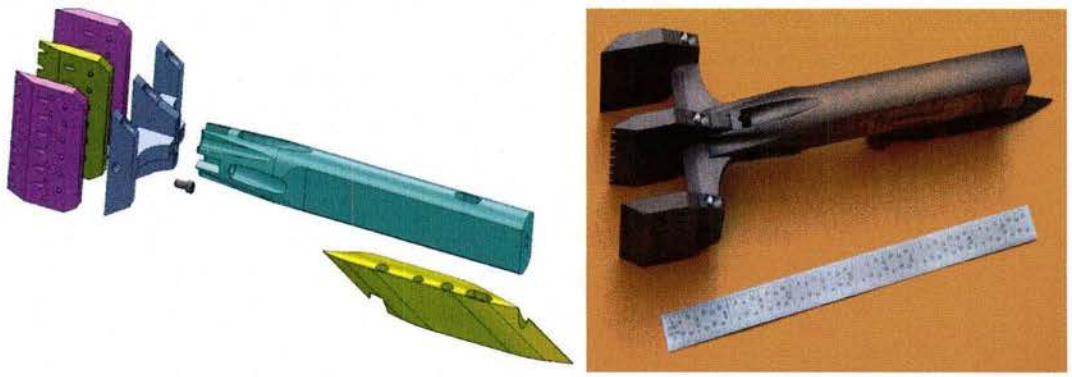

Fig. 10. The newly developed 5×8 thermocouple rake array holder. Left: Computer-design model. Right: Stanless-steel assembly produced using rapid-prototyping fabrication.

This part of the experimental work was begun by Michael Johnson, who was followed by Jeff Bergthorson and Aris Bonanos, and continued by Luca Maddalena as the lead

investigator up and until the end of this grant. Starting in October 2009, Prakhar Mehrotra joined the research group as a graduate student. He had the opportunity to overlap with Luca Maddalena, undergoing 8 weeks of training on laboratory operating procedures and safety engineering before Dr. Maddalena's departure from Caltech at the end of November 2009 to assume his responsibilities at the University of Texas at Arlington.

Numerical simulations

An accompanying computational effort focused on simulations of the flow field and turbulent mixing in the expansion ramp injection geometry and jets into a supersonic cross-stream. The simulations utilize large-eddy simulation with subgrid scale modeling techniques (LES–SGS) to represent the physics of the unresolved scales. The computational framework developed as part of the Caltech ASC DoE program (Pantano *et al.* 2007) was used for all simulations. The computational framework has adaptive mesh refinement (AMR) capability, employs advanced low-dissipation finite-difference discretizations with shock-capturing capabilities in supersonic flows, in combination with the stretched-vortex LES–SGS model of Pullin and co-workers (e.g., Misra & Pullin 1997, Voelkl, Pullin & Chan 2000; Pullin 2000; Pullin & Lundgren 2001), and the ghost-fluid method for the application of boundary conditions in complex geometries. Prior to the simulation of turbulent flows, the numerical solver was subjected to a thorough verification program (Matheou 2008, Matheou *et al.* 2008).

Simulations corresponding to the experiments in the expansion ramp injection geometry with a subsonic top stream show that the flow and mixing predictions of the LES are in good agreement with experimental measurements. The recirculating flow between the ramp and the reattachment of the shear layer is reproduced by the LES (Fig. 11, between bottom wall and bottom green layer). The magnitude of the velocity of upstream-moving flow near the lower wall is 10–15% of the top free stream velocity for mass injection ratios of about 1/10 but becomes negligible as the flow tends towards a free-shear layer for higher mass-injection ratios of about 1/5. The agreement in the pressure coefficient profiles along the top and bottom walls and the total pressure profiles along the transverse direction is satisfactory.

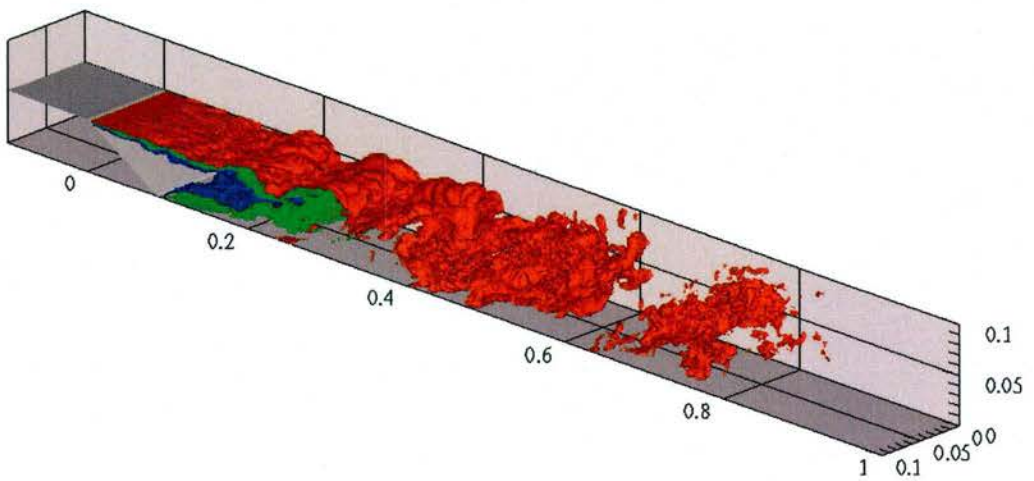

Fig. 11. Instantaneous isosurfaces of mixture fraction, Z, in the LES of turbulent mixing in the expansion-ramp configuration with a subsonic top stream ($M_1 = 0.3$). Three isosurfaces are plotted at $Z = 0.2$, 0.5 and 0.8. The top stream carries a value of $Z = 1$ and the bottom $Z = 0$.

Total (resolved-scale plus subgrid contribution) probability density functions (PDFs) of mixture fraction were estimated using a presumed beta-distribution model for the subgrid field. The PDF shapes illustrate the improved mixing characteristics of the expansion-ramp geometry, compared to free-shear layers at equivalent conditions. Computed mixing statistics were found to be in good agreement with the experimental measurements, with no adjustments necessary, indicating that mixing on a molecular scale is predicted correctly by the LES–SGS model developed.

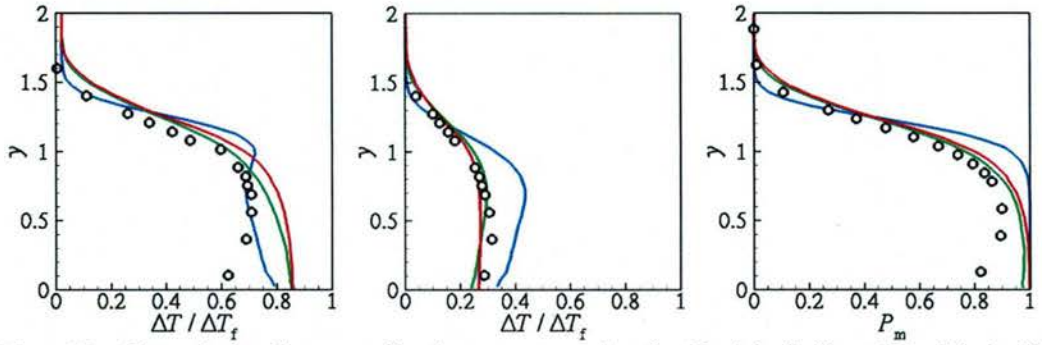

Fig. 12. Plots depict the normalized temperature rise for H_2-rich (left) and F_2-rich (middle) chemically reacting flow conditions, and the probability profile of mixed fluid (right). Symbols correspond to experimental measurements and lines to LES at three grid-resolutions: fine (red), medium (green) and low resolution (blue). Profiles are plotted along the transverse (vertical) direction, y, at the location of the measurement rake about $x = 6$ half-duct heights downstream of the ramp-injection.

Flow-statistics were found to be resolution-independent by computing the flow at three grid resolutions, at two and four times the resolution of the coarsest simulation. Figure 12 shows a comparison of the mixing statistics between experiments and simulations. LES results are seen to converge at the two highest grid resolutions used and match the experimental measurements, except near the lower wall, where the absence of wall and turbulent boundary layer modeling did not allow flow separation effects to be captured. The statistical variability observed between the cases simulated was shown to be attributable to differences in LES predictions rather than insufficient statistical convergence, as discussed in Matheou *et al.* (2010).

Overall, the LES predictions reproduced the observed flow field and elucidated characteristics of the flow that are difficult to measure. For the first time, grid-convergence was demonstrated for a LES of passive mixing in a complex flow. This work is part of the graduate and postdoctoral research of Georgios Matheou.

LES–SGS of an inclined circular jet (helium at $M_j = 1$) into a supersonic turbulent boundary layer (air at $M_\infty = 3.6$) also was performed. In the present numerical investigation, the jet geometry and flow parameters matched those in the experiments of Maddalena *et al.* (2006) with a single injector. The numerical study of Ferrante *et al.* (2009) showed that the main flow features generated by the gas dynamic interactions of an inclined jet with a supersonic cross-flow, such as the barrel shock, Mach disk, shear layer, and the counter-rotating vortex pair, are captured numerically by the LES–SGS modeling framework. However, the transition and spatial development of the helium jet were shown to be strongly dependent on the cross-flow inflow conditions. These results indicate that correct turbulent inflow conditions are required for reliable predictions of the dispersion and mixing of a gaseous jet in a supersonic, turbulent cross-flow.

A novel methodology for the generation of synthetic turbulent inflow conditions for LES of spatially-developing, supersonic, turbulent wall-bounded flows has been developed (Ferrante *et al.* 2010) based on the approach of Ferrante & Elghobashi (2003). This approach was applied to the study of a supersonic turbulent flow over a flat wall interacting with an inclined jet (Ferrante *et al.* 2010), as illustrated in Fig. 13. This work was part of the postdoctoral research of Antonino Ferrante (currently Assistant Professor at the University of Washington). The fluid dynamics video "LES of an inclined jet into a supersonic turbulent crossflow" shows five animations (A1 to A5) that can be downloaded (Ferrante *et al.* 2009v):

A1. Mach-number, M, contours in the mid-span plane;

A2. contours of density-gradient magnitude in the mid-span plane;

A3. isosurface of helium mass-fraction, $Y_{He} = 0.25$;

A4. isosurface of λ_2 (vortical structures);

A5. overlapped isosurface of helium mass-fraction $Y_{He} = 0.25$ (yellow), and vortical structures (blue).

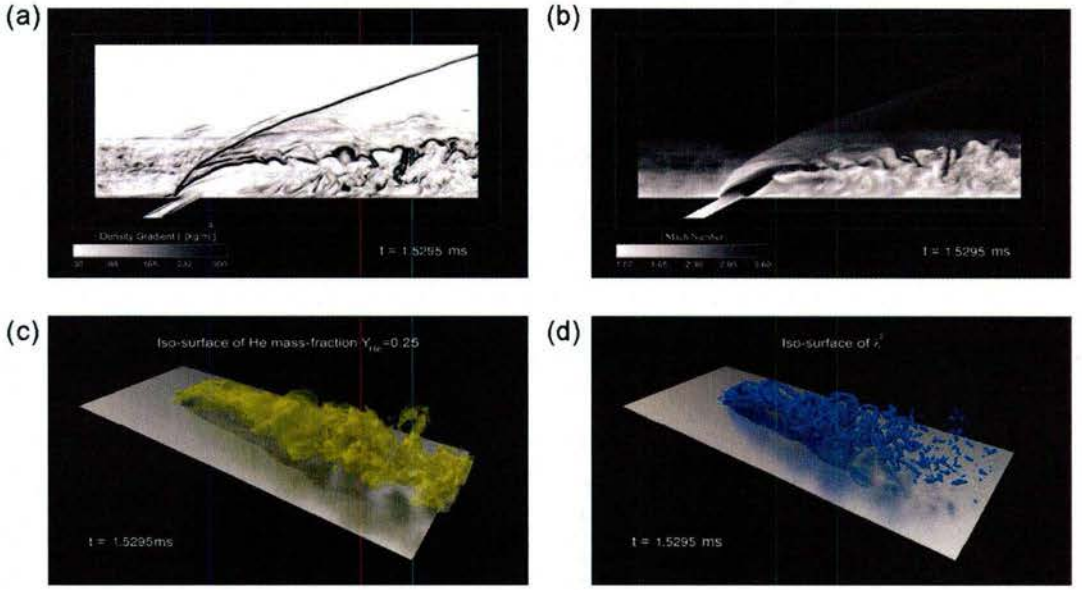

Fig. 13. (a) Instantaneous density-gradient magnitude in the mid-span plane; (b) instantaneous Mach number in the mid-span plane; (c) instantaneous $Y_{He} = 0.25$ helium mass-fraction isosurface; (d) instantaneous vortical structures identified with the λ_2 method (Jeong & Hussain 1995).

Each animation lasts about 23 s at 30 fps for a total of 696 frames. The temporal development of the flow is shown for about 10^{-3} s. Thus, the flow is shown 23,000 times slower than would occur in real time. Instantaneous frames from the animation are shown in Fig. 13.

Mach number contours (A1) show that boundary-layer the interaction between the turbulence and the bow shock produces shock-wave unsteadiness that affects the roll-up of the shear-layer (formed between air stream and helium jet) and, consequently, modulates in time the size and shape of the barrel shock (black region near the jet exit). The contours of the density gradient magnitude (A2) show the bow shock and the shear-layer formed in between the air stream after the bow shock and the expanded helium jet.

Both contours show large-scale structures that are advected downstream. Jet unsteadiness, lateral and wall-normal helium dispersion, and three-dimensional structure of the helium jet are shown in the animation of $Y_{He} = 0.25$ isosurface (A3). The vortical structures (isosurface of λ_2 shown in A4) are sheets near the jet exit where the shear formed between the air stream and the helium jet is large. Downstream the jet exit, the vortical structures are mostly tilted tubes that sometimes look like discontinuous rings. In A5, the isosurface of $Y_{He} = 0.25$ (yellow) mostly envelopes the isosurface of λ_2 (blue). The two isosurfaces, showing helium-jet puffs and vortical structures, are well correlated in space and time. The vortical structures look like muscles that move the isosurface of helium mass-fraction, contributing to helium dispersion and the convoluted helium mass fraction isosurface. Both computational efforts (ramp and jet) were in collaboration with Carlos Pantano, at the University of Illinois at Urbana-Champaign. The images in Fig. 13 were generated by Paul Adams and his group at the Data Analysis and Assessment Center, U.S. Army Engineer Research and Development Center (HPCMP/DoD), MS 39180, USA. (Ferrante *et al.* 2010).

Hydrocarbon combustion and flames

Work on hydrocarbon combustion under this grant focused on laminar, premixed high-pressure methane-air flames and atmospheric methane-air, ethane-air, ethylene-air, propane-air, and propylene-air flames.

Benezech *et al.* (2009) showed that the comparison of high-quality axial velocity and CH-radical profile measurements in strained premixed flames stabilized in a jet-wall stagnation flow can be used to validate and compare chemical-kinetic mechanisms, and applied this methodology to C_1-C_2 hydrocarbon flames. They also showed that flame location provides a good surrogate for flame speed in this configuration. See also Sone (2007).

Benezech (2008) and Benezech *et al.* (2009) extended the measurements to C_3 hydrocarbon flames and implemented a new particle tracking velocimetry (PTV) technique that improved spatio-temporal resolution of velocity measurements. Experimental data were compared with the results of simulations performed with the CANTERA reacting-flow software package. The simulations rely on a one-dimensional hydrodynamic model, a multi-component transport formulation including thermal diffusion, and several detailed chemical kinetic mechanisms. The kinetic models used in Benezech (2008) and Benezech *et al.* (2009) are GRI-MECH 3.0 (referred as G3) by Smith *et al.*; the C_3 mechanism by Davis, Law, and Wang (1999), hereafter referred as DLW; the latest (2005/12) release of the C_1-C_3 San-Diego mechanism (S5); the C_3 mechanism of Battin-Leclerc *et al* (Gueniche *et al.* 2006), referred as BL; and the C_1-C_3 Konnov (2000) mechanism (KON). A novel continuation technique between mechanisms was developed to obtain solutions with the less-robust BL and KON mechanisms.

In most practical applications, including anticipated scramjet propulsion applications, combustion takes place at elevated pressures. Pressure affects the combustion kinetics, with the relative importance of two-body versus three-body reactions decreasing with increasing pressure. As a result, reaction paths are pressure-dependent and high-pressure kinetics cannot be inferred based on models validated with atmospheric-pressure data. There is a dearth of validation data at elevated pressures.

To remedy this deficiency, the development of the variable pressure flame facility (VPFF) was begun under the sponsorship of this grant at Caltech that allows

measurements in laminar, axisymmetric, premixed, stagnation flames while dynamically controlling the pressure in the range from 0.1 to 12 atmospheres.

As part of the work sponsored by this grant, C_3H_8- and C_3H_6-air flames were investigated experimentally at p = 1 atm. Figure 14 compares experimental PTV axial velocity, u, and CH-PLIF profiles with numerical predictions based on DLW in a stoichiometric propane-air flame. The chemistry seems modeled adequately by DLW in this flame. The modeled PT profile (Benezech 2008) accurately captures the shape of the experimental velocity profile, even within the flame region where steep gradients occur, as well as in the vicinity of the wall.

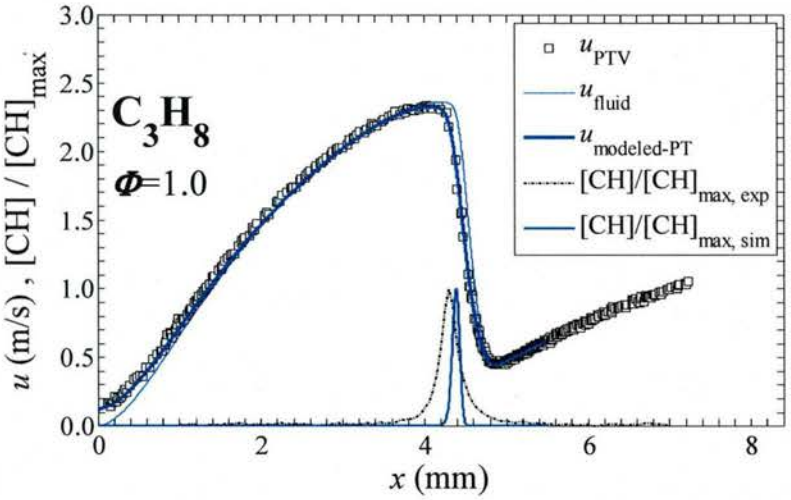

Fig. 14. Φ = 1.0 C_3H_8-air flame profiles simulated using the DLW mechanism.

Figure 15 shows the difference between the predicted CH-profile peak location, $x_{CH,sim}$, and the measured CH-profile peak location, $x_{CH,exp}$, scaled by the stoichiometric CH-layer thickness simulated with S5, i.e., $\delta_{CH,S5,\Phi=1}$. Positive values of $(x_{CH,sim} - x_{CH,exp}) / x_{CH,S5,\Phi=1}$ indicate that the simulated CH profile is centered upstream of the measured profile and, by inference, that simulated flame speed is higher than measured flame speed. Figure 15 also shows that S5 and BL are the best mechanisms to use to simulate the C_3H_8 and C_3H_6 flames investigated, respectively, but that there is a systematic variance between C_3H_6 flame predictions and experiment with increasing equivalence ratio. Except for the very rich C_3H_6 flame (for which flame speeds are overpredicted by all the mechanisms tested), BL and KON predict similar results in C_3H_8 and C_3H_6 flames. Better agreement was found in C_3H_8 flames for DLW and S5. Nevertheless, DLW and S5 show larger variation with experiment in C_3H_6 flames. This finding suggests that reaction pathways for the (unsaturated) C_3H_6 may be missing in DLW and S5 that are present in the larger reaction-number mechanisms BL and KON (Benezech 2008, Benezech *et al.* 2009).

In the newly developed flame facility, the gas delivery system (Fig. 16) is equipped with high-accuracy Coriolis mass flow meters, MicroMotion CMF010 for air and MicroMotion LF2M for fuel, with NIST-traceable accuracy of 0.35% and 0.5%, respectively. These meters allow monitoring the fuel-air mixture equivalence ratio with high precision, as required to reduce uncertainty in the fuel-air mixture composition and equivalence ratio.

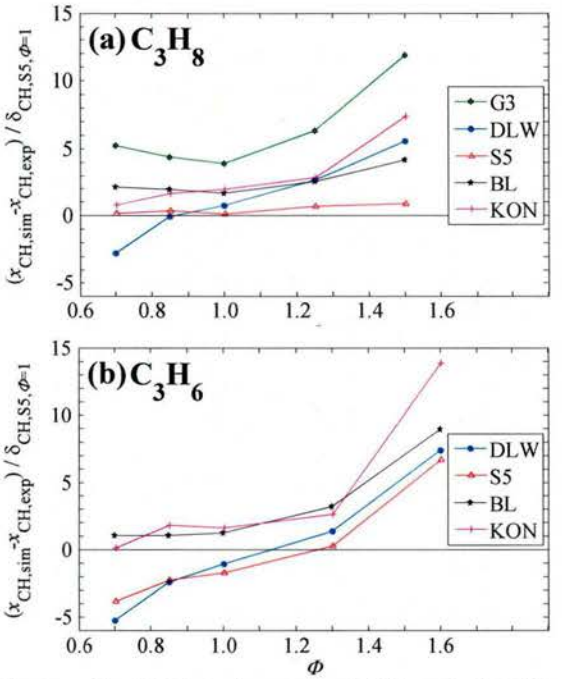

Fig. 15. Differences between simulated and measured CH-peak locations for: (a) C_3H_8-air and (b) C_3H_6-air flames (C_3H_6 is not included in the G3 mechanism).

Co-flow plena, nozzles, and a stagnation plate developed for atmospheric-pressure flames (Bergthorson 2005) are installed in a pressure vessel (Fig. 17) that is pressurized by inert gas. The chamber pressure is controlled dynamically with a PID controller in a back-pressure configuration (Alicat Scientific PCR-300PSIA-D) and monitored with a high-accuracy pressure transducer (Omega PX1K1-300AI). Temperatures of the fuel-air mixture nozzle and of the stagnation plate are monitored with K-type thermocouples. A data-acquisition system (National Instrument cDAQ-9178 chassis with NI 9203 module) records the data generated by these instruments.

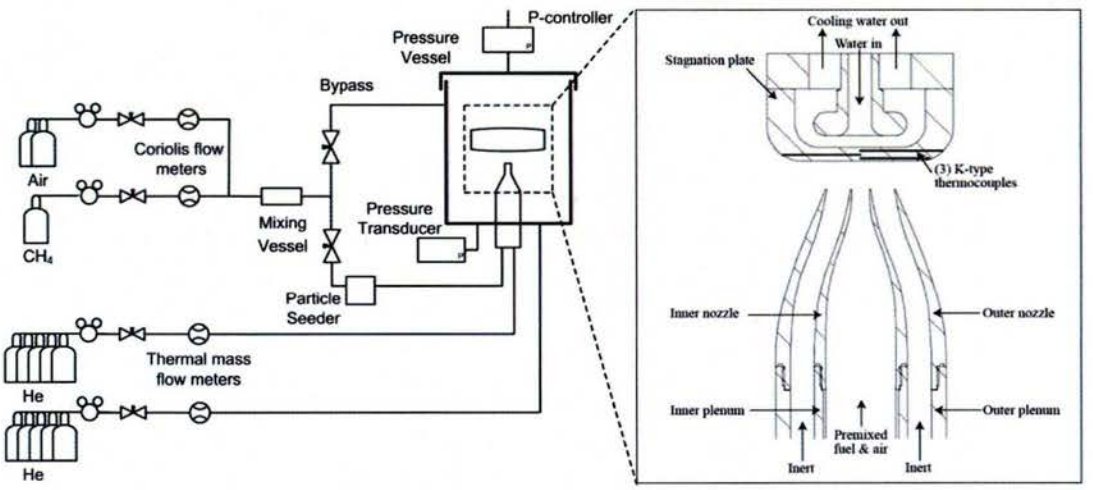

Fig. 16. Simplified schematic of the Variable Pressure Flame Facility, showing only the gas delivery and pressure control systems.

The pressure vessel has a cylindrical inner chamber (30cm diameter × 40cm height) and an octagonal outer shell. The latter allows the cameras used for PTV and PLIF to be at a 135° angle from each other (Fig. 17), preventing direct line-of-sight between cameras and enabling simultaneous PTV and PLIF measurements.

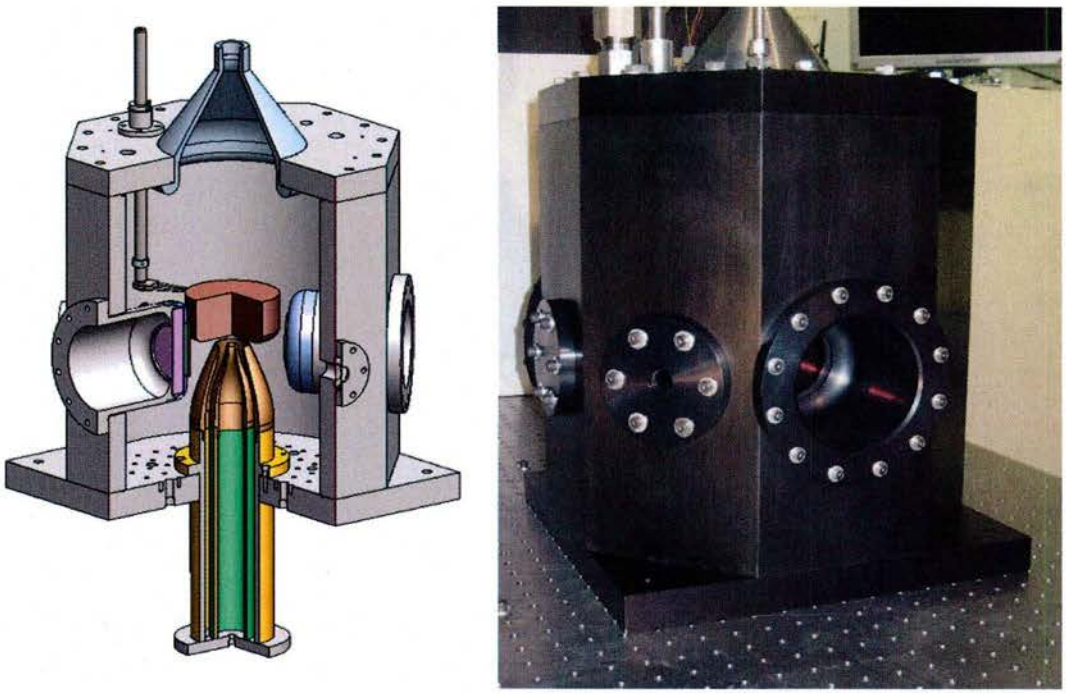

Fig. 17. Octagonal pressure vessel. Left: cutaway computer design model showing co-flow plena and nozzles, and stagnation plate inside the chamber. Right: photo of final chamber. Orange reflections in the view port are from the heat-blocking mirror installed in it.

Experiments and optical measurements at atmospheric pressure can be conducted in an open facility that requires no windows. At high pressure, however, laser and optical access must be provided through windows that impose challenges. All windows in the Variable Pressure Flame Facility are made of fused silica, which has a low coefficient of thermal expansion and a high tolerance to thermal shock, as well as good transmittance in the near UV where the PLIF measurements are made. Two large view ports allow the cameras to be positioned as closely as possible from the flame, maximizing the viewing solid angle and therefore the signal recorded by the cameras. Due to the close proximity of the camera port windows to the flame, heat-reflecting mirrors (Precision Glass Optics HRM) blocks IR radiation from the flame, keeping the fused silica windows cool and reducing the risk of window failure.

Measurements in high-pressure flames are challenging for various reasons: cellular and pulsating instabilities in the flame front produce unsteadiness (Law 2006), enhanced aerooptical effects complicate and compromise optical diagnostics, and soot-formation is (thermodynamically) favored at higher pressures. While the latter could, in principle, be included in the kinetics and overall modeling, the maturity of soot physics is not as far along and would compromise the validation of single-phase gas kinetics that is the aim of these experiments. To assess those effects in our geometry, PTV measurements along the flame axis were conducted to determine applicable operational limits.

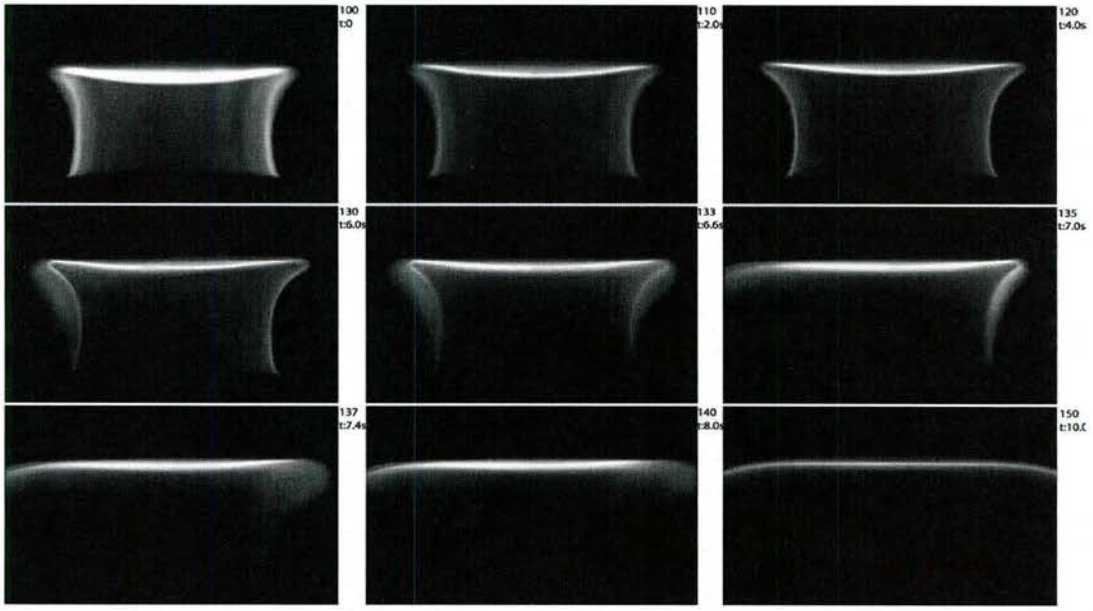

Fig. 18 CH_4-air flame start up sequence at p = 5 atm. Cellular instabilites at Φ=0.85 (upper left photo) are overcome by decreasing Φ to 0.75. In the last photo of the sequence the flame edges are detached from the nozzle and a stable flat flame is obtained. The sequence duration is 10s.

At pressures greater than 5 atm, cellular instabilities can appear in the flame. However, the flame transitions through a hysteresis cycle and stable flat-flame operation can be achieved at low strain rates by initially decreasing the equivalence ratio to that of a very lean mixture. Once a flat flame is established, the equivalence ratio can be increased to the values of interest, while the flame remains stable (Fig. 18).

The pressure and temperature dependence of a pure gas refractive index is modeled by the Gladstone-Dale coefficient, β_o, defined by the relation (e.g., Dimotakis *et al.* 2001),

$$n_{gas} - 1 = \beta_o \frac{P}{P_o} \frac{T_o}{T},$$

where T_0 and P_0 are a reference temperature and pressure, respectively. This dependence of the index of refraction on pressure – on number density, to be more exact – illustrates the expected increasing importance of aerooptical effects with increasing pressure. For $p > 5$ atm using, the previous gas mixtures, aerooptical aberrations can blur the flame front location (Fig. 19). These effects can be mitigated using helium as a diluent and buffer gas. In particular, cold helium has a refractive index within 2×10^{-4} of that of the flame at elevated pressures and yields good results when used both as a co-flow and background chamber gas (Fig. 20). Figure 20 also shows that flames can be stable at a pressure of 5 atm and that aerooptical effects at high pressures can be mitigated significantly by such means.

Stable flame operation has been demonstrated to pressures in excess of 5 atm. PLIF and PTV measurements are presently in progress over a range of pressures up to 5 atm and beyond, and combustion kinetics and transport models are being tested against this data using the CANTERA reacting-flow simulation package.

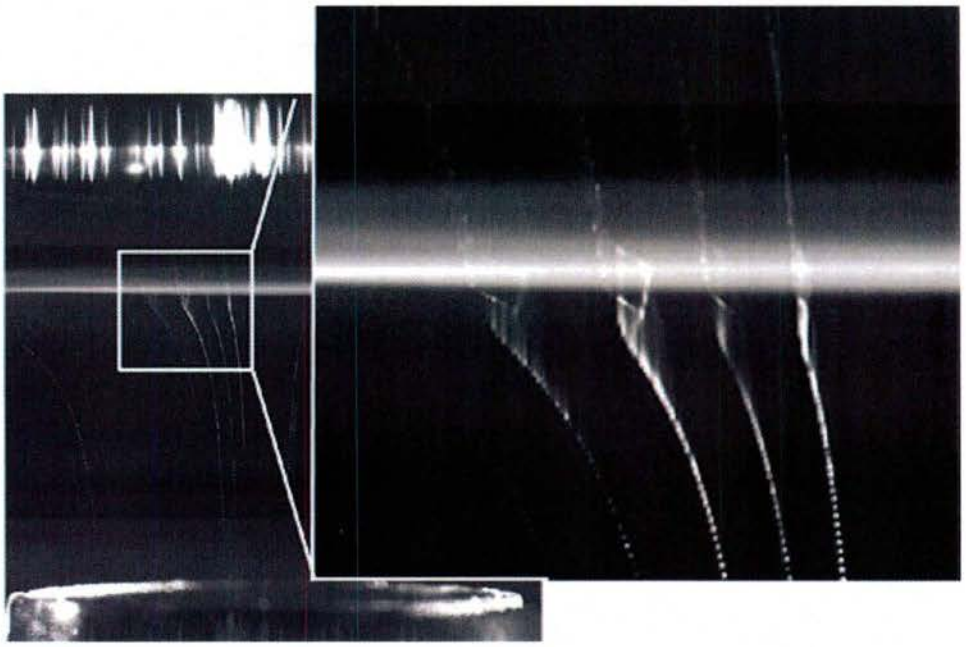

Fig. 19 Illustration of aerooptical effects. CH_4-air flame, p = 6 atm, Φ = 0.80 with N_2 used for both the co-flow and background gas. PTV trajectories are blurred by differences in refractive index between the flame and surrounding gases.

This part of the work was begun as the graduate and post-doctoral research of Jeff Bergthorson, continued as part of the graduate research of Laurent Benezech, and is conducted as part of the post-doctoral research of Philippe Bardet as the lead investigator.

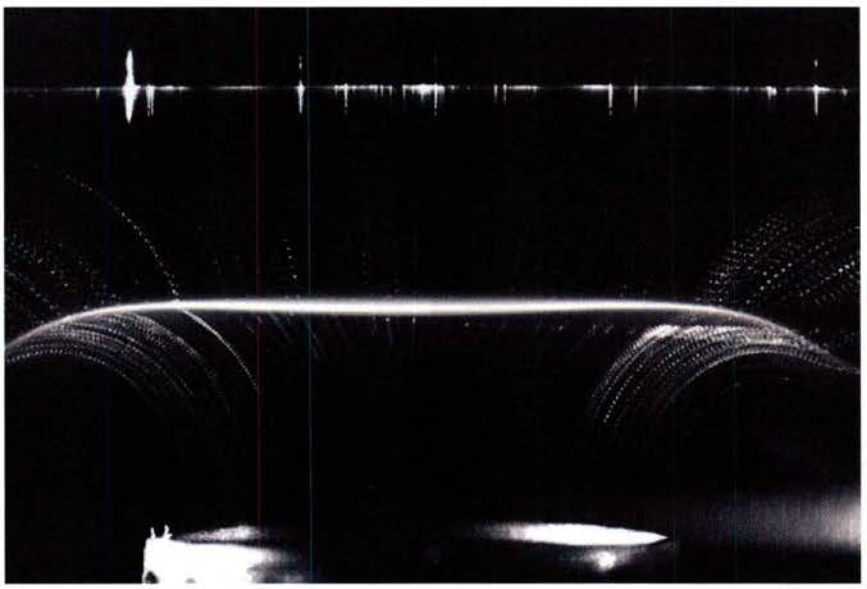

Fig. 20 CH_4-air, p = 5 atm, Φ = 0.85, with He as both the co-flow and background gas. Aerooptical effects are mitigated allowing quantitative PTV trajectory measurements.

Experiments at this writing are in progress at pressures between 1 and 7 atmospheres that focus on refining flame investigation diagnostics (PTV and PLIF) at elevated pressures.

They are proceeding under support provided by the Caltech Northrop Chair and the Caltech Provost.

Scalar dispersion in turbulent flows

The injection of fuel in a high-speed combustor couples with the flow dynamics in many ways. For its primary purpose, injection provides the supply of fuel to be burned with the air stream. Secondarily, however, injection details play a major role in the entrainment, dispersion, and resulting mixing. The discussion on high-speed mixing above documented the experimental and numerical simulation work undertaken to investigate mixing and mixing enhancement in internal flows of relevance to high-speed propulsion. The investigations discussed below aim to address specific issues that arise with respect to momentum added or subtracted in the course of the injection and its consequences on dispersion and mixing. The experimental work undertaken as part of this grant is also a precursor to investigations of mixing in a stratified fluid (in a gravitational field) that provides a dynamic equivalent to mixing in fluid parcels across density interfaces in a Lagrangian acceleration field, as occurs in mixing of (high-density) injected fuel with the (lower-density) air stream. While the experiments described below investigate scalar dispersion and mixing in grid turbulence in incompressible flow, several issues are expected to be generic and to provide guidance for designing and optimizing the more complex flows that arise in real air-breathing combustor applications.

The specific experiments undertaken include fundamental studies of dispersion of a conserved scalar marker released from a simulated point source at a controlled distance downstream of a turbulence-generating grid. Grid turbulence is a well-studied flow and remains the closest experimental realization (e.g., Comte-Bellot & Corrsin 1966, Mydlarski & Warhaft 1996, and others) of the homogeneous isotropic turbulence assumptions under which the main theories were developed (Kolmogorov 1941a, 1941b; Monin & Yaglom 1975). Scalar dispersion in uniform density grid turbulence also provides an important benchmark against which dispersion in more complex flows can be compared.

Theoretical progress in this flow was contributed by George (1992) in terms of his equilibrium-similarity analysis. This theory proposes that a large number of flows admit self-preserving solutions that are valid at all scales of the flow. In the particular case of decaying homogeneous isotropic turbulence, the decay rate of the kinetic energy is of power-law form and, according to George (1992) can depend on initial/inflow conditions, so that decay-rate constants need not be universal except, possibly, in the limit of 'infinite' Reynolds number. Most experiments reported do not cover a sufficiently large range of initial/inflow conditions or a wide-enough range of Reynolds numbers and decay (Lagrangian) times to validate these proposals. A short range of realized decay times, along with measurement sampling rates that were achieved in previous work, lead to large uncertainties of the estimated power-law decay range (Mohamed & Larue 1990, Lavoie *et al.* 2007).

Our experiments were designed to overcome these and other shortcomings. The quasi-homogeneous and isotropic turbulent flow produced by a grid with a wire size of ¼" and 1" wire spacing (mesh size) was towed through a tank with stationary optics, camera, and mean flow (Fig. 21). This allows recording of the scalar (non-buoyant) plume from its initial development to the latter stages of the decay of turbulence. This configuration also allows the Reynolds number dependence of the scalar dispersion to be investigated, with

a range of initial Taylor Reynolds numbers, Re_T, spanning the (mixing) transition at $Re_T \sim 70\text{-}80$ (Dimotakis 2000, 2005). The grid is moved by a computer-controlled gear-motor that ramps it up to speed at the start of the run, maintains a constant speed through the center region and ramps it down at the end of the run. Reynolds numbers based on mesh size can be varied in the range of $320 < Re_M < 56{,}000$.

The measurements rely on laser-induced fluorescence (LIF), with data recorded using a high-speed, low-noise, high frame-rate digital-imaging CCD-based camera that has been developed in-house (Kern *et al.* 2005, Sec. 2.G). The scalar field can be investigated over a wide range of dilutions ($1{:}10^4$-10^5 is not uncommon in our experiments), in either two or three dimensions as a function of time. A quad, high-power, pulsed (200 Hz) Nd:YAG laser system (custom-built by Spectra-Physics) is used for the light source. The Nd:YAG laser produces a pulsed output of approximately 8 ns duration, so the exposure time is negligible compared to the camera CCD readout time, obviating separate shuttering wasting no light during CCD readout.

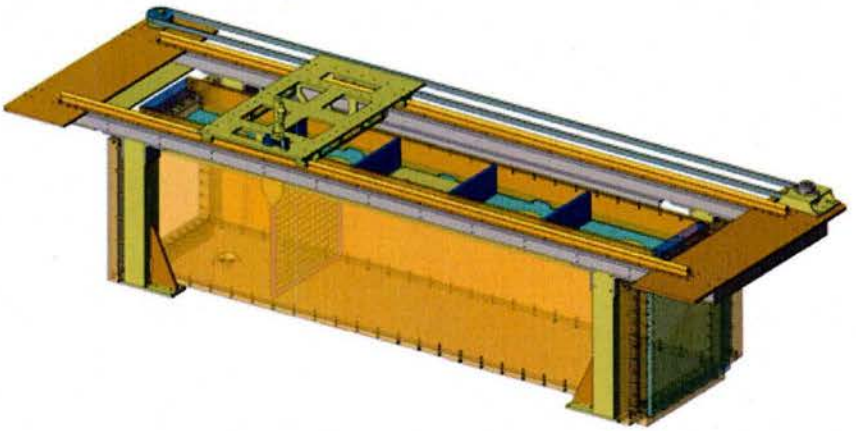

(a) Tow-tank and computer-controlled motorized grid

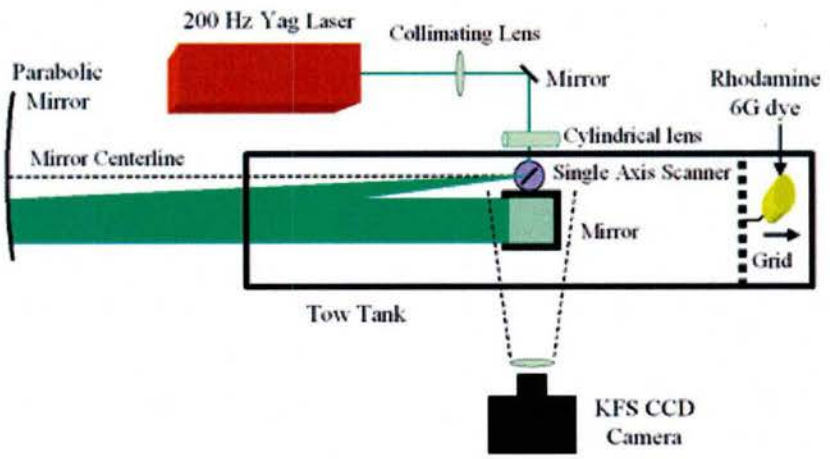

(b) Experiment schematic (top view).

Fig. 21. Tow-tank schematics for the scalar-dispersion experiments (unpublished).

A cylindrical lens forms the laser beam into a sheet while a galvanometrically driven scanner optionally allows stepping/sweeping the sheet perpendicular to itself through the test section. This optical configuration achieved through the use of an astronomical-quality ($\lambda/8$), large-aperture parabolic mirror and laser sheet virtual origin placed at the mirror's focus to collimate the sheet, making the laser slices parallel to each other. Rhodamine 6G dye is used to match the 532 nm wavelength of the frequency-doubled Nd:YAG laser. A small amount of dye is premixed in the tank provides full-frame shot-to-shot laser-intensity calibration and correction. The temperature field is kept constant and uniform in the tank to avoid stratification and buoyancy effects that will be investigated, separately, in future work.

Single 2-D vertical slices, either parallel or perpendicular to the scalar injector, are recorded as a function of Reynolds number and dye-injection details. This ability to span large ranges in both Reynolds number and scalar concentration elucidated previously uncovered behavior, especially as regards initial-condition effects, as discussed below.

The passive scalar is introduced from a point source (small, hypodermic tubing) just downstream of the grid at three controlled momentum-flux conditions:

- a momentum-less-wake condition in which the momentum injected with the scalar matches the momentum loss generated by the tube (Fig. 22, black lines),
- a wake (momentum-defect) condition (Fig. 22, blue line), and
- a jet (momentum-excess) condition (Fig. 22, red line).

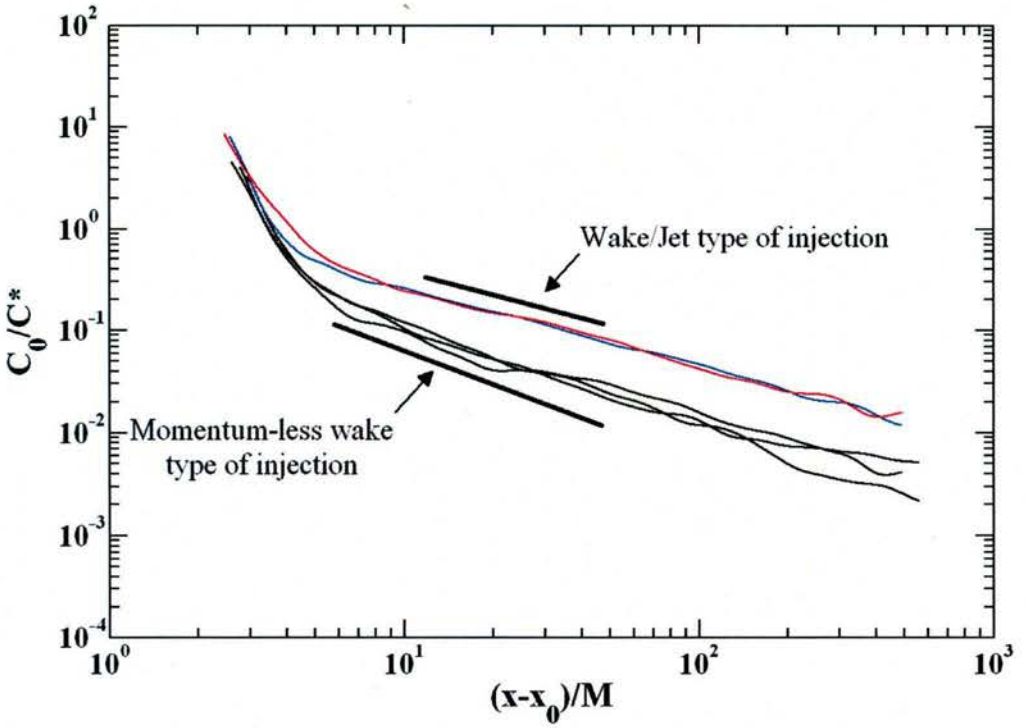

Fig. 22. Downstream variation of the normalized centerline mean concentration for three types of scalar injection and a mesh Reynolds number of Re_M = 56,000. Black lines: momentumless wake. Blue line: (momentum-defect) wake. Red line: (momentum-excess) jet. M is the grid mesh size (here, 1″). The virtual origin x_0, and C^* are the power-law fitting parameters. Unpublished work by Krawczynski *et al.* (in preparation).

Data compiled in this figure derive from streamwise cuts (transects) of the scalar field, with a laser sheet plane that includes the injector. Using fitting parameters to extract the power law decay range parameters, the downstream variation of the centerline mean concentration C_0, decreases approximately classically as the reciprocal of the downstream distance, $C_0 \sim x^{-1}$ for the momentum-matching case (Fig. 22, black lines). Jet or wake injection conditions also exhibit a power law far-field decay range, with $C_0 \sim x^{-2/3}$, as expected for such flows, i.e., a *slower* decay/mixing than for momentumless injection. The difference in behavior can be understood because injection momentum excess or defect leads to different far-field behavior and, because momentum must be conserved, the dispersion characteristics are altered throughout the flow field, i.e., this kind of initial condition cannot be "forgotten" by the flow. The "memory" of the initial conditions is retained even though the disturbance caused by the injection is small compared to the fluctuations of the (background) grid turbulence. In other words, the jet/momentum-less/wake nature of the injection determines the scalar plume behavior and the resulting self-similar dispersion properties.

The acquisition of instantaneous 3-D scalar field data (multiple vertical slices) in a later phase will allow characterization of the structures of the concentration field and their comparison to local turbulence properties and produce multi-dimensional space-time data for modeling and code validation including subgrid scale (SGS) modeling.

The new research effort will extend these investigations to stable non-uniform-density flows to explore mixing across stably stratified interfaces in 1 g acceleration and simulate mixing across stable interfaces in a (Lagrangian) accelerating frame. The experiments will make use of extensions to the diagnostics that were used for the data described in this report to permit laser beams to cross density interfaces with minimal optical distortion.

This part of the work was executed by Jean-Francois Krawczynski as the lead investigator. The fast-framing camera, special optics, and computer-controlled technology and data acquisition development were led by Daniel Lang, who is continuing these investigations.

References

BARBER, M.J., J.A. SCHETZ, L.A. ROE 1997 Normal, Sonic Helium Injection Through a Wedge- Shaped Orifice into Supersonic Flow. *J. Propulsion and Power*, 13(2).

BEN-YAKAR, A., M. G. MUNGAL, AND R. K. HANSON 2006 Time Evolution and Mixing Characteristics of Hydrogen and Ethylene Transverse Jets in Supersonic Crossflow. *Physics of Fluids, Vol. 18.*

BENEZECH, L.J. 2008 *Premixed hydrocarbon stagnation flames: experiments and simulations to validate combustion chemical-kinetic models*. Engineer thesis, California Institute of Technology.

BENEZECH, L.J., J.M. BERGTHORSON, AND P.E. DIMOTAKIS 2009 Premixed laminar C_3H_8- and C_3H_6-air stagnation flames: experiments and simulations with detailed kinetic models. *Proceedings of the Combustion Institute* 32:1301-1309.

BERGTHORSON, J.M. 2005 *Experiments and Modeling of Impinging Jets and Premixed Hydrocarbon Stagnation Flames*. Ph.D. thesis, California Institute of Technology.

BERGTHORSON, J.M., M.B. JOHNSON, A.M. BONANOS, AND P.E. DIMOTAKIS 2007 Measurements of Molecular Mixing in an Expansion-Ramp Combustor. *21st ICDERS*, Poitiers, France.

BONANOS, A., J. BERGTHORSON, AND P.E. DIMOTAKIS 2008 Mixing Measurements in a Supersonic Expansion-Ramp Combustor. *Flow, Turbulence and Combustion* 80:489-506.

COMTE-BELLOT, G., AND S. CORRSIN 1966 The use of a contraction to improve the isotropy of grid-generated turbulence. *J. Fluid Mech.* 25:657–682.

DAVIS, S.G., LAW, C.K., AND H. WANG 1999 Propene pyrolysis and oxidation kinetics in a flow reactor and laminar flames. *Combust. & Flame* 119:375–399.

DIMOTAKIS, P.E. 2000 The mixing transition in turbulent flow. *J. Fluid Mech.* 409:69–98.

DIMOTAKIS, P.E. 2005 Turbulent mixing. *Ann. Rev. Fluid Mech.* 37:329–56.

DIMOTAKIS, P.E., H.J. CATRAKIS, AND D.C. FOURGUETTE 2001 Flow structure and optical beam propagation in high-Reynolds-number gas-phase shear layers and jets. *J. Fluid Mech.* 433:105-134.

FERRANTE, A. AND S.E. ELGHOBASHI 2004 A robust method for generating inflow conditions for direct simulations of spatially-developing turbulent boundary layers. *J. Comp. Physics* 198:372-387.

FERRANTE, A., G. MATHEOU, P.E. DIMOTAKIS, M. STEPHENS, P. ADAMS, AND R. WALTERS 2009v LES of an inclined jet into a supersonic turbulent cross-flow. Download PDF, Download High-Resolution Video, Download Low-Resolution Video, arXiv:0910.3018v1 *Gallery of Fluid Motion, APS-DFD* (Minneapolis, MN).

FERRANTE, A., G. MATHEOU, AND P.E. DIMOTAKIS 2010 LES of an Inclined Jet into a Supersonic Turbulent Crossflow: Synthetic Inflow Conditions. *48th AIAA Aerospace Sciences Meeting, AIAA-2009-1511*

FERRANTE, A., C. PANTANO, G. MATHEOU, AND P.E. DIMOTAKIS 2009 On the Effects of the Upstream Conditions on the Transition of an Inclined Jet into a Supersonic Cross-Flow. *47th AIAA Aerospace Sciences Meeting,* AIAA-2009-1511.

FERRANTE, A., C. PANTANO, G. MATHEOU, AND P.E. DIMOTAKIS, M. STEPHENS, P. ADAMS, R. WALTERS, AND R. HAND 2008 LES of an Inclined Jet into a Supersonic Cross-Flow. *arXiv:0810.1957v1*.

GEORGE, W.K. 1992 The decay of homogeneous isotropic turbulence. *Phys. Fluids* A 4(7):1492–1509.

GUENICHE, H.A., P.A. GLAUDE, G. DAYMA, R. FOURNET, AND F. BATTIN-LECLERC 2006 Rich methane premixed laminar flames doped with light unsaturated hydrocarbons i. allene and propyne. *Combust. & Flame* 146:620–634.

JEONG, J. AND F. HUSSAIN 1995 On the identification of a vortex. *J. Fluid Mech.* 285:69–94.

JOHNSON, M.B. 2005 *Aerodynamic Control and Mixing with Ramp Injection.* Engineer's thesis, California Institute of Technology.

KERN, B., P.E. DIMOTAKIS, C. MARTIN, D.B. LANG, AND R.N. THESSIN 2005 Imaging through turbulence with a quadrature-phase optical interferometer. *Appl. Optics* 44:7424-7438.

KOLMOGOROV, A.N. 1941a The local structure of turbulence in incompressible viscous fluid for very large Reynolds numbers. *Dokl. Akad. Nauk. SSSR* 30:301–305.

KOLMOGOROV, A.N. 1941b Dissipation of energy in locally isotropic turbulence. *Dokl. Akad. Nauk. SSSR* 32:16–18.

KONNOV, A.A. 2000 Detailed reaction mechanism for small hydrocarbons combustion. Version 0.5 available at <http://homepages.vub.ac.be/_akonnov/>.

KRAWCZYNSKI, J.F., D.B. LANG, AND P.E. DIMOTAKIS 2010 Scalar dispersion in uniform-density grid turbulence (in preparation).

LAVOIE, P., L. DJENIDI, AND R.A. ANTONIA 2007 Effect of initial conditions in decaying turbulence generated by passive grids. *J. Fluid Mech.* 585:395–420.

LAW, C.K. 2006 Propagation, structure, and limit phenomena of laminar flames at elevated pressures. *Comb. Sc. & Tech.* 178:335-360.

MADDALENA, L., T.L. CAMPIOLI, AND J.A. SCHETZ 2006 Experimental and computational investigation of light-gas injectors in Mach 4.0 crossflow. *J. Propulsion & Power* 22:1027–1038.

MADDALENA, L., S. HOSDER, A. BONANOS, AND P.E. DIMOTAKIS 2008a Extended Conical Flow Theory for Design of Pressure Probes in Supersonic Flows. *47th AIAA Aerospace Sciences Meeting, AIAA-2009-1072*.

MADDALENA, L., J.A. SCHETZ, AND R. NEEL 2008b Vortex Interactions with a Jet in a Supersonic Crossflow. *46th AIAA Aerospace Sciences Meeting* (Reno, NV).

MATHEOU, G., A.M. BONANOS, C. PANTANO, AND P.E. DIMOTAKIS 2009 Large-eddy simulation of turbulent mixing in a recirculating shear flow. *J. Fluid Mech.* 646:375–414.

MATHEOU, G. 2008 *Large-Eddy Simulation of Turbulent Mixing in a Recirculating Shear Flow*. Ph.D. Thesis California Institute of Technology.

MATHEOU, G., C. PANTANO, AND P.E. DIMOTAKIS 2008 Verification of a fluid-dynamics solver using linear stability results. *J. Comp. Phys.* 227(11):5385–5396.

MATHEOU, G. 2008 *Large-Eddy Simulation of Turbulent Mixing in a Recirculating Shear Flow*. Ph.D. Thesis California Institute of Technology.

MATHEOU, G., A.M. BONANOS, C. PANTANO, AND P.E. DIMOTAKIS 2010 Large-Eddy Simulation of Turbulent Mixing in a Recirculating Shear Flow. *J. Fluid Mech.* 646:375-414.

MATHEOU, G., C. PANTANO, AND P.E. DIMOTAKIS 2008 Verification of a Fluid-Dynamics Solver Using Linear Sability Results. *J. Comp. Phys.* 227(11):5385–5396.

MISRA, A. & D.I. PULLIN 1997 A vortex-based subgrid stress model for large-eddy simulation. *Phys. Fluids* 9:2443–2454.

MOHAMED, M., AND J. LARUE 1990 The decay power law in grid-generated turbulence. *J. Fluid Mech.* 219:195–214.

MONIN, A.S., AND A.M. YAGLOM 1975 *Statistical Fluid Mechanics*. Vol. 2. MIT Press.

MUNGAL, M. AND P.E. DIMOTAKIS 1984 Mixing and Combustion With Low Heat Release in a Turbulent Shear Layer. *Physics of Fluids*.12(7):1629-1645.

MYDLARSKI, L., AND Z. WARHAFT 1996 On the onset of high Reynolds number grid generated wind tunnel turbulence. *J. Fluid Mech.* 320:331–368.

PANTANO, C., R. DEITERDING, D.J. HILL AND D.I. PULLIN 2007 A Low Numerical Dissipation Patch-Based Adaptive Mesh Refinement Method for Large-Eddy Simulation of Compressible Flows. *J. Comp. Phys.* 221(1):63–87.

PULLIN, D. I. 2000 A vortex-based model for the subgrid flux of a passive scalar. *Phys. Fluids* 12:2311–2316.

PULLIN, D. I. & T.S. LUNDGREN 2001 Axial motion and scalar transport in stretched spiral vortices. *Phys. Fluids* 13:2553–2563.

San Diego mechanism, Center for Energy Research (Combustion Division), University of California at San Diego. available at <http://maeweb.ucsd.edu/_combustion/cermech/>.

SANTIAGO, J.G., AND J.C DUTTON. 1997 Velocity Measurements of a Jet Injected into a Supersonic Crossflow, *J. Propulsion and Power*, 13(2).

SEINER, J.M., S.M. DASH, AND D.C. KENZAKOWISKI 2001 Historical Survey on Enhanced Mixing in Scramjet Engines. *J. Propulsion & Power* 17:1273-86.

SMITH, G.P., D.M. GOLDEN, M. FRENKLACH, N.W. MORIARTY, B. EITENEER, M. GOLDENBERG, C.T. BOWMAN, R.K. HANSON, S. SONG, W.C. GARDINER, V.V. LISSIANSKI, AND Z. QIN Gri-mech 3.0. available at <http://www.me.berkeley.edu/gri mech/>.

SONE, K. 2007 *Modeling and Simulation of Axisymmetric Stagnation Flames*. Ph.D. thesis, California Institute of Technology.

VOELKL, T., D.I. PULLIN & D.C. CHAN 2000 A physical-space version of the stretched-vortex subgrid-stress model for large-eddy simulation. *Phys. Fluids* 12:1810–1825.

Personnel

Bardet, Philippe: Post-Doctoral Scholar in Aeronautics, Caltech.

Bergthorson, Jeffery: Graduate Research Assistant and Post-Doctoral Scholar, Aeronautics, Caltech. Presently, Assistant Professor, McGill University, Canada.

Bonanos, Aristides: Postdoctoral Scholar in Aeronautics, Caltech. Presently, Associate Research Scientist, The Cyprus Institute, Cyprus.

Dahl, Earl: Member of the Technical Staff, Aeronautics, Caltech. Presently, retired, part-time consultant.

Dimotakis, Paul (PI): John K. Northrop Professor of Aeronautics and Professor of Applied Physics, Caltech, and Chief Technologist, JPL.

Ferrante, Antonino: Postdoctoral Scholar in Aeronautics, Caltech. Presently, Assistant Professor, U. Washington.

Lang, Daniel: Research Engineer, Aeronautics, Caltech.

Maddalena, Luca: Postdoctoral Scholar in Aeronautics, Caltech. Presently, Assistant Professor, U. Texas at Arlington.

Matheou, George: Graduate Research Assistant, and Postdoctoral Scholar in Aeronautics, Caltech and, presently, Member of the Technical Staff, Jet Propulsion Laboratory.

Mehrotra, Prakhar, Graduate Research Assistant in Aeronautics, Caltech.

Meiron, Daniel (Co-PI): Fletcher Jones Professor of Applied and Computational Mathematics and Computer Science, Caltech.

Mojahedi, Christina: Administrative Assistant, Aeronautics, Caltech.

Valiferdowsi, Bahram: Member of Technical Staff, Aeronautics, Caltech.

Support provided to all personnel listed above by this grant was part time.

Other collaborators:

Deiterding, Ralph: Senior Postdoctoral Scholar in Applied and Computational Mathematics, Center for Advanced Computing Research, Caltech.

Goodwin, David: Professor Mechanical Engineering and Appl. Physics, Caltech. Author of the *Cantera* software package and collaborator on DNS of hydrocarbon flames.

Hill, David: Postdoctoral Scholar, Aeronautics, Caltech.

Pantano, Carlos: Assistant Professor, Mechanical Engineering, U. Illinois, Urbana-Champagne.

Pullin, Dale: Theodore von Kármán Professor of Aeronautics, Caltech.

Publications of work supported under this grant

Refereed publications supported under this grant

Bergthorson, J.M., M.B. Johnson, A.M. Bonanos, M.D. Slessor, W. Su, and P.E. Dimotakis 2008 Molecular mixing and flowfield measurements in a recirculating shear flow. Part I: subsonic flow. *Flow, Turbulence and Combustion* 83(2):153-303.

Bonanos, A., J. Bergthorson, and P.E. Dimotakis 2008 Mixing measurements in a supersonic expansion-ramp combustor. *Flow, Turbulence and Combustion* 80:489-506, doi:10.1007/s10494-008-9133-7.

Bonanos, A.M., J.M. Bergthorson, and P.E. Dimotakis 2008 Molecular mixing and flowfield measurements in a recirculating shear flow. Part II: supersonic flow. *Flow, Turbulence and Combustion* 83(2):251-268.

Ferrante, A., C. Pantano, G. Matheou, and P.E. Dimotakis, M. Stephens, P. Adams, R. Walters, and R. Hand 2008 LES of an inclined jet into a supersonic cross-flow. *arXiv:0810.1957v1*.

Grossman, P., L. Maddalena, and J. Schetz 2007 Wall injectors for high Mach number scramjets. *J. Propulsion and Power* 24(2):259-266.

Maddalena, L., T. Campioli, and J. Schetz 2006 Experimental and computational investigation of light gas injectors in Mach 4.0 cross flow. *J. Propulsion and Power* 22(5):1027-38.

Matheou, G. 2008 Large-eddy simulation of molecular mixing in a recirculating shear flow. *Ph.D. thesis, California Institute of Technology*.

Matheou, G., A.M. Bonanos, C. Pantano, and P.E. Dimotakis 2010 Large-Eddy Simulation of Turbulent Mixing in a Recirculating Shear Flow. *J. Fluid Mech.* . 646:375–414.

Matheou, G., C. Pantano, P.E. Dimotakis 2008 Verification of a fluid-dynamics solver using correlations with linear stability results. *J. Comp. Physics* 227:5385-5396.

Pantano, C., D.I. Pullin, P.E. Dimotakis, and G. Matheou 2008 LES approach for high Reynolds number wall-bounded flows with application to turbulent channel flow. *J. Comp.* 227(21):9271–9291.

Conference papers supported under this grant

Bergthorson, J.M., A.M. Bonanos, M.B. Johnson, and P.E. Dimotakis 2008 Measurements of molecular mixing in high-speed flows using fast chemistry. *Proc. 2008 Spring Technical Meeting of the Combustion Institute/Canadian Section.*

Bergthorson, J.M., M.B. Johnson, A.M. Bonanos, and P.E. Dimotakis 2007 Measurements of molecular mixing in an expansion-ramp combustor. *Proc. 21st International Colloquium on the Dynamics of Explosions and Reactive Systems*, Poitiers, France.

Bonanos, A.M., L. Maddalena, and P.E. Dimotakis 2008 Observations on a supersonic shear layer. *47th AIAA Aerospace Sciences Meeting, AIAA-2009-26.*

Bonanos, A., J.M. Bergthorson, and P.E. Dimotakis 2007 Molecular mixing and flowfield measurements in an expansion-ramp combustor: supersonic flow. *43rd AIAA/ASME/SAE/ASEE Joint Propulsion Conference & Exhibit, AIAA-2007-5417.*

Campioli, T., L. Maddalena, and J. Schetz 2006 Studies of shock wave/transverse injection interaction on supersonic mixing processes. *AIAA-2006-8135.*

Ferrante, A., C. Pantano, G. Matheou, and P.E. Dimotakis 2009 On the effects of the upstream conditions on the transition of an inclined jet into a supersonic cross-flow. *47th AIAA Aerospace Sciences Meeting AIAA-2009-1511.*

Maddalena, L., S. Hosder, A. Bonanos, and P. Dimotakis 2008 Extended conical flow theory for design of pressure probes in supersonic flows. *47th AIAA Aerospace Sciences Meeting, AIAA-2009-1072.*

In preparation

Bardet P. M., and Dimotakis, P. E. 2010 Premixed laminar C1-C2 stagnation flames: experiments and simulations at elevated pressures (in preparation).

Interactions/Transitions

P.E. Dimotakis discussed scramjet design and mixing with Dr. Campbell Carter of AFRL.

New discoveries, inventions, or patent disclosures

Maddalena L., A. M. Bonanos, P. E. Dimotakis and A. Ferrante 2008 *A High-spatial-resolution probe, with a simplified calibration technique for simultaneous total and static pressure measurements in supersonic flow with moderate flow angularity and swirl.* US Provisional Application No. 29,373 (Filed in 2008)

Lifetime Honors and Awards

In reverse chronological order:

Honor/Award: Fellow Year received: 2010
Honor/Award Recipient(s): Dimotakis, Paul E.
Awarding Organization: American Institute of Aeronautics & Astronautics

Honor/Award: Fellow Year received: 2008
Honor/Award Recipient(s): Dimotakis, Paul E.
Awarding Organization: AAAS

Honor/Award: Associate Fellow Year received: 1989
Honor/Award Recipient(s): Dimotakis, Paul E.
Awarding Organization: American Institute of Aeronautics & Astronautics

Honor/Award: Fellow Year received: 1980
Honor/Award Recipient(s): Dimotakis, Paul E.
Awarding Organization: American Physical Society

Student theses or dissertations supported under this grant

Author: **Benezech, Laurent**
Affiliation: *California Institute of Technology*
Type of document: Engineer's thesis (2008)
Title: *Premixed hydrocarbon stagnation flames: experiments and simulations to validate combustion chemical-kinetic models.*
http://resolver.caltech.edu/CaltechETD:etd-05302008-113043

Author: Matheou, Georgios
Affiliation: California Institute of Technology
Type of document: Ph.D. dissertation (2008)
Title: *Large-eddy simulation of molecular mixing in a recirculating shear flow.*
http://resolver.caltech.edu/CaltechETD:etd-05262008-152803

Author: **Sone, Kazuo**
Affiliation: *California Institute of Technology*
Type of document: Ph.D. thesis (2007)
Title: *Modeling and simulation of axisymmetric stagnation flames.*
http://resolver.caltech.edu/CaltechETD:etd-04252007-170838